Dynamics of a contact process with ontogeny

Joshua S. Weitz[1,2,*] and Daniel H. Rothman[1,†]
[1]*Department of Earth, Atmospheric, and Planetary Sciences, Massachusetts Institute of Technology, Cambridge, Massachusetts 02139, USA*
[2]*Department of Physics, Massachusetts Institute of Technology, Cambridge, Massachusetts 02139, USA*
(Received 11 September 2003; revised manuscript received 18 May 2004; published 31 August 2004)

We propose a simple model of how sessile organisms grow, disperse, and die. Our model extends the contact process to include a spatially explicit representation of organismal growth in addition to the familiar terms denoting reproduction and mortality. We develop a size-structured mean field theory which predicts an oscillatory phase as a consequence of excess reproduction. Monte Carlo simulations of a spatial implementation show instead a transition from a dilute to a ring-like phase. The ring-like phase arises as a consequence of the competition for limited space among juvenile and mature organisms, i.e., the ecological cost of reproduction. We also calculate the phase transition between life and death in the spatial model and find that it is in the same universality class as directed percolation. Finally, we analyze the onset of the ring-like phase via a spatial autocorrelation and comment on the model's applicability to problems in the study of ecosystem structure and dynamics.

DOI: 10.1103/PhysRevE.70.021915 PACS number(s): 87.23.Cc, 64.60.Ht, 05.70.Fh, 02.50.Ey

I. INTRODUCTION

The contact process is one of the simplest examples of a system exhibiting a nonequilibrium phase transition [1–4]. It was originally developed as a model of the spread of epidemics [5] for which disease dynamics depend upon contact. More recently, the contact process and its variants have been applied to the study of spatial ecologies [6–8] where the behavior of sessile organisms such as plants and trees are modeled as lattice particles which can disperse, compete, and die. However, even at the most coarse grained level, the life cycle of a plant involves dispersal, competition, death, as well as growth. As is obvious to anyone who has tried to grow a vegetable garden, "the commonest fate of plants under natural conditions is to die before reaching reproductive maturity [9]." In this paper, we introduce a class of contact process models which include the period of ontogeny during which organisms grow from juveniles to adults capable of reproduction.

In order to incorporate organismal growth into the contact process, we begin by defining the model in terms of generalized dispersal and growth mechanisms. We attempt throughout this paper to retain the analogy with the simple contact process as much as is possible. Thus far, limited work has demonstrated how structured populations may impact spatial phenomena such as disease spreading [10,11] and the fluctuations of population density in pelagic communities [12]. Applications of size-structured theory to the dynamics of plants and trees [13–15] have generally been limited to nonspatial models; however, see Ref. [16] for an empirically based alternative.

We begin by introducing a mean field version of the contact process with ontogeny, which we solve, finding the phase boundary between death, life, and an oscillating steady state. We then implement a spatially explicit version of the model using Monte Carlo simulations in the continuum. The size-structured model in its spatially explicit form generates a surprising array of patterns (see Fig. 4 for examples). These patterns include ring-like structures of juveniles surrounding a central or absent adult. As we will demonstrate, the development of these structures stems from the mutual inhibition of growth via competition for limited local space.

Our aim in investigating the spatial implementation of the model is twofold: (i) To characterize the phase transition between life and death and (ii) to demonstrate the failure of mean field theory to capture the ecologically meaningful behavior of the system far from the persistence–extinction phase boundary. We also point out a number of ways in which this model may be applied to studies of size-structured plant communities.

II. GENERAL MODEL OF A CONTACT PROCESS FOR GROWING PARTICLES

In the lattice contact process, an individual lattice site may be occupied ($\eta=1$) or unoccupied ($\eta=0$). Every occupied site "dies" ($\eta=1\rightarrow 0$) at a rate m and creates an offspring at a rate c which is then deposited on a randomly selected nearest neighbor. Only those offspring that are deposited on an empty site survive, which is a consequence of limiting sites to, at most, single occupancy. A mean field theory of the system is derived by assuming that all sites are connected and that there are no spatial correlations. The interested reader may refer to the book by Marro and Dickman [3] for details on the difference between mean field theory and spatial implementations of the model.

The dynamics of a contact process with ontogeny reflects a period during which the particle grows from a juvenile to

*Present address: Department of Ecology and Evolutionary Biology, Princeton University, Princeton, NJ 08544; electronic address: jsweitz@princeton.edu
†Electronic address: dan@segovia.mit.edu

an adult. In our conception of the process, every particle has a d-dimensional center $\mathbf{x}_i$, radius r_i, and a size-structured fecundity rate, $c(r)$. Particles are sessile, die at a rate $m(r)$, cannot overlap, and grow larger (when unimpeded) with velocity $G_i(t-t_i)$ where t_i is the birth time. As our intention is to mimic the contact process as closely as possible, we assume that organisms only reproduce once they reach their maximum adult size, r_a, i.e.,

$$c(r) = c\delta(r - r_a), \tag{1}$$

where c is the dispersal rate. We also choose a size-independent mortality rate, $m(r)=m$. Offspring are deposited randomly along the locus of points located a distance $2r_a$ away from $\mathbf{x}_i$. Competition arises as a consequence of particle collisions. The simplest case is one of hard-core interactions, i.e., particle collisions leads to temporary cessation of growth. For numerical simulation of such a model, we keep track of the number of neighbors, n_i, and restrict growth to those particles for which $r<r_a$ and $n_i=0$. Alternative models will be addressed in Sec. V.

The dynamics of the simple contact process depends on the ratio of dispersal rate to mortality rate, $\lambda \equiv c/m$, as well as the size L and dimension d of the lattice. For a contact process with ontogeny, the dynamics also depend on the ratio between growth rate to mortality rate. For linear growth, $G_i(t-t_i)=\epsilon$, we may write such a ratio as

$$\theta = \frac{\epsilon}{(r_a - r_0)m}. \tag{2}$$

This ratio sets a dimensionless time delay, $\tau = 1/\theta$, in the dynamics as will be explained in the derivation of the mean field theory in the following section.

III. MEAN FIELD THEORY

In the contact process without ontogeny, the overall density ρ behaves, in the mean field approximation, like [3]

$$\frac{d\rho}{dt} = \lambda\rho(1-\rho) - \rho. \tag{3}$$

This result leads to the stability condition, $\lambda > 1$, which separates the extinction equilibrium, $\rho^* = 0$, from the persistence equilibrium, $\rho^* = 1 - \lambda^{-1}$. The analysis of the contact process with ontogeny is far more complicated. We begin by deriving the "equations of motion" for $\rho(r,t)$, the density of particles of size r at time t. We then show how suitable integrations over the equations of motion lead to a set of coupled time delay differential equations describing the behavior of macroscopic variables, such as overall number density and fraction of adults. Using these macroscopic differential equations, we are able to derive formulas describing the nontrivial persistence equilibrium. We then perform linear stability analysis on the fixed points of the system, calculating the phase diagram in the space of (θ,λ), and demonstrating the presence of an additional phase where oscillations are to be expected. We restrict our analysis throughout the sections that follow to the case of two-dimensional systems, i.e., those most often applied to the dynamics of plants and trees.

A. Equations of motion for a size-structured theory

Recall for a moment the definition of the model outlined in Sec. II. In the contact process with ontogeny, organisms grow from a minimum size r_0, at birth, to a maximum size r_a, at maturity. In order to fully describe the behavior of the size-structured population, we will need to derive equations of motion for the change in density of organisms with radii $r_0 < r < r_a$. We will also need appropriate boundary conditions that link the adult population to the birth of new organisms. Without loss of generality, we assume $r_0=0$ and $r_a=1$.

There are two important points relevant to the analysis that follows. The first is that we assume the impact of a spatially limited process is to restrict the birth of new particles in a density-dependent fashion. We do not however explicitly incorporate spatial limitations in the growth of particles after they are born. Extending the present mean field theory to include the impact of particle collisions, even in an approximate sense, would be particularly useful. The second point is that although r denotes the radius of the particles, it is technically analogous to an age insofar as we allow particles to grow beyond $r_a=1$. However, for the purposes of calculating area, all particles with $r>1$ are assigned the radius $r=1$.

If $\rho(r,t)\Delta r$ is the number density of organisms with radii between r and $r+\Delta r$ at time t, then

$$\rho(r, t+\Delta t)\Delta r = \rho(r - \epsilon\Delta t, t)\Delta r(1 - m\Delta t), \tag{4}$$

where $1-m\Delta t$ is the probability that a particle does not die in a time period Δt. Expanding both sides of Eq. (4) to first order yields

$$\frac{\partial \rho(r,t)}{\partial t} + \epsilon\frac{\partial \rho(r,t)}{\partial r} + m\rho(r,t) = 0. \tag{5}$$

This equation describes a decaying wave in radius-space and is a standard form when analyzing age- and size-structured populations [17–19]. What distinguishes Eq. (5) from equations describing the propagation of physical waves is the nonlocal coupling of $\rho(0,t)$ to the density of mature organisms,

$$\rho(r=0,t)\Delta r = c(1 - A(t))\int_{t-\Delta r/\epsilon}^{t} dt'(1 - m(t-t'))\int_1^\infty dr\rho(r,t'), \tag{6}$$

where the fractional area taken up by organisms is [41]

$$A(t) = \int_0^1 \mathrm{d}r\,\pi r^2 \rho(r,t) + \int_1^\infty \mathrm{d}r\,\pi\rho(r,t). \tag{7}$$

When $A(t) > 1$, then $\rho(r=0,t)=0$; this is the effect of space limitation. Integrating Eq. (6) over t' yields the number density of births,

$$\rho(r=0,t) = \frac{c(1-A(t))}{\epsilon}\int_1^\infty \mathrm{d}r\rho(r,t). \tag{8}$$

Along with the initial conditions, $\rho(r,t=0)=f(r)$, we now have a full set of equations describing the size-structured population in a mean field sense. For ease of reference, the equations are

$$\begin{aligned} &\frac{\partial\rho(r,t)}{\partial t} + \epsilon\frac{\partial\rho(r,t)}{\partial r} + m\rho(r,t) = 0, \\ &\rho(r=0,t) = \frac{c(1-A(t))}{\epsilon}\int_1^\infty \mathrm{d}r\rho(r,t), \\ &\rho(r,t=0) = f(r). \end{aligned} \tag{9}$$

Solving for $\rho(r,t)$ requires a choice of initial conditions, $f(r)$. As time increases, it is clear that the impact of initial conditions steadily dissipates. But how may we make such a statement quantitative? Note that any particles with radius $r \geqslant \epsilon t$ at time t must be relics of the initial distribution. Whereas, any particles with radius $r < \epsilon t$ must have been born after the evolution of the system began. Thus, given a size-independent mortality rate m, we may write

$$\rho(r,t) = \begin{cases} e^{-mr/\epsilon}\rho(0,t-r/\epsilon), & r < \epsilon t, \\ e^{-mt}f(r-\epsilon t), & r \geqslant \epsilon t. \end{cases} \tag{10}$$

At this point, we may solve the system using one of two techniques [20–22]: (i) Substituting the steady-state value of $\rho(r,t)$ in Eq. (10) into Eq. (8) and then solving for a self-consistent $\rho(r=0,t)$ from which the other quantities may be derived, or (ii) integrating over the equation of motion (5) in various ways to deduce the relationship between macroscopic variables, such as area, birth rate, total number density, etc., from which the fixed points and their stability may be derived. We choose to follow the second path as it appears, to us, to be the more intuitive means to explain the system dynamics.

B. Dynamics of macroscopic indicators

Thus far, we have made reference to "macroscopic indicators" but we have not yet stated which variables are necessary to fully describe the dynamics of the system. In Table I, we list the relevant variables that we will make use of in the course of this analysis. We begin by considering the evolution of $p(t)$, the overall density, which we find by integrating Eq. (5) from $r=0$ to $r=\infty$,

TABLE I. A list of macroscopic indicators for the mean field theory of contact processes with ontogeny.

Variable	Definition	Property
$p(t)$	$\int_0^\infty \mathrm{d}r\rho(r,t)$	Overall density
$p_a(t)$	$\int_1^\infty \mathrm{d}r\rho(r,t)$	Density of adults
$A_j(t)$	$\int_0^1 \mathrm{d}r\,\pi r^2\rho(r,t)$	Area of juveniles
$S_j(t)$	$\int_0^1 \mathrm{d}r 2\pi r\rho(r,t)$	Perimeter of juveniles
$p_j(t)$	$p(t)-p_a(t)$	Density of juveniles
$A(t)$	$A_j(t)+\pi p_a(t)$	Overall area
$R(t),\rho(0,t)$	$c(1-A(t))p_a(t)/\epsilon$	Birth rate

$$\int_0^\infty \mathrm{d}r\left(\frac{\partial\rho(r,t)}{\partial t} + \epsilon\frac{\partial\rho(r,t)}{\partial r} + m\rho(r,t)\right) = 0. \tag{11}$$

Because $\rho(r\to\infty,t)\to 0$,

$$\begin{aligned} p'(t) &= \epsilon R(t) - mp(t), \\ &= c(1-A(t))p_a(t) - mp(t). \end{aligned} \tag{12}$$

Likewise, the evolution of $p_a(t)$ is found by integrating Eq. (5) from $r=1$ to $r=\infty$,

$$\begin{aligned} p_a'(t) &= \epsilon\rho(1,t) - mp_a(t), \\ &= \epsilon e^{-m/\epsilon}R(t-1/\epsilon) - mp_a(t), \end{aligned} \tag{13}$$

where we may make use of Eq. (10) to replace $\rho(1,t)$. Because $A(t)$ may be expressed in terms of $A_j(t)$ and $p_a(t)$, we now multiply Eq. (5) by πr^2 and integrate from $r=0$ to $r=1$ to find

$$\begin{aligned} A_j'(t) &= -\pi\epsilon\rho(1,t) + \epsilon S_j(t) - mA_j(t), \\ &= -\pi\epsilon e^{-m/\epsilon}R(t-1/\epsilon) + \epsilon S_j(t) - mA_j(t), \end{aligned} \tag{14}$$

where the integration involving $r^2\partial\rho(r,t)/\partial r$ is done by parts. Finally, by multiplying Eq. (5) by $2\pi r$ and integrating from $r=0$ to $r=1$ we find the evolution of $S_j(t)$,

$$\begin{aligned} S_j'(t) &= -2\pi\epsilon\rho(1,t) + 2\pi\epsilon p_j(t) - mS_j(t), \\ &= -2\pi\epsilon e^{-m/\epsilon}R(t-1/\epsilon) + 2\pi\epsilon(p(t)-p_a(t)) \\ &\quad - mS_j(t). \end{aligned} \tag{15}$$

These four equations, (12)–(15), constitute a complete set of coupled, time-delay differential equations which we may use to find the steady-state behavior of the model. It is worthwhile to write the complete set of equations together, rewriting $R(t)$ in terms of $p_a(t)$ and $A_j(t)$. In addition, we will also nondimensionalize time, $t\to mt$, and incorporate the two dimensionless parameters, λ and θ, denoting the relative importance of reproduction and growth to mortality, respectively. The equations are

$$
\begin{aligned}
p'(t) &= \lambda(1 - A_j(t) - \pi p_a(t))p_a(t) - p(t), \\
p_a'(t) &= \lambda e^{-1/\theta} p_a(t-\tau)(1 - A_j(t-\tau) - \pi p_a(t-\tau)) - p_a(t), \\
A_j'(t) &= -\pi\lambda e^{-1/\theta} p_a(t-\tau)(1 - A_j(t-\tau) - \pi p_a(t-\tau)) + \theta S_j(t) - A_j(t), \\
S_j'(t) &= -2\pi\lambda e^{-1/\theta} p_a(t-\tau)(1 - A_j(t-\tau) - \pi p_a(t-\tau)) + 2\pi\theta(p(t) - p_a(t)) - S_j(t).
\end{aligned}
\tag{16}
$$

C. Definitions of the steady states

The fixed points of the system are found by setting the time derivatives of Eq. (16) to zero. Besides the extinction equilibrium, there is also a nontrivial fixed point which, after some algebraic manipulation, may be expressed as

$$A^* = \frac{\lambda - e^{1/\theta}}{\lambda}, \tag{17}$$

$$R^* = \frac{A^*}{c(\theta)}, \tag{18}$$

$$p^* = \theta R^*, \tag{19}$$

$$p_a^* = \theta e^{-1/\theta} R^*, \tag{20}$$

$$A_j^* = A^* - \pi\theta e^{-1/\theta} R^*, \tag{21}$$

$$S_j^* = A^*/\theta, \tag{22}$$

where the constant $c(\theta)$ is defined as

$$c(\theta) = 2\pi\theta^3 - 2\pi\theta^3 e^{-1/\theta} - 2\pi\theta^2 e^{-1/\theta}.$$

We verify the steady-state predictions using an explicit time difference solver of Eq. (9) with 10^2 grid points in radius space. In Fig. 1, we confirm dependence of A^* on λ for $\theta=5$ and $0 \leqslant \lambda \leqslant 10$. Note that the fixed point only exists when $\lambda > e^{1/\theta}$. For values of λ slightly above this cutoff, $A^*(\lambda) \propto \lambda$, the same dependence that the contact process retains in the mean field theory (3) for λ just greater than 1.

D. Linear stability of the extinction equilibrium

The stability criteria of the extinction equilibrium where $\rho^*(r)=0$ is already apparent from the form of Eq. (17). Because there are only two fixed points in the system, we expect the absorbing state to be unstable whenever $\lambda > e^{1/\theta}$. In principle, this condition may be found via a linear stability analysis of Eq. (16). Instead, we offer a heuristic derivation of this stability criteria.

We posit that the system will go extinct if, on average, the number of offspring a new organism generates is less than 1. If this is the case, then perturbations that render the system nearly vacant, for which space is not a limitation, will drive the system even further toward extinction. The average number of expected offspring of a newly seeded particle is

$$
\begin{aligned}
N_0 &= [\text{Probability of surviving to maturity}] \\
&\quad \times [\text{Average offspring of an adult}], \\
&= e^{-1/\theta}\lambda.
\end{aligned}
\tag{23}
$$

Hence, the condition $N_0 > 1$ is satisfied when $\lambda > e^{1/\theta}$.

E. Linear stability of the persistence equilibrium

The stability of the nontrivial fixed point is difficult to calculate in a closed form because of the time-delay nature of Eq. (16). We proceed, pointing out when numerical analysis must be used to determine stability for a given parameter set.

Consider a general system of time-delay differential equations,

$$\frac{d\mathbf{x}}{dt} = \mathbf{F}(\mathbf{x}(t), \mathbf{x}(t-\tau)), \tag{24}$$

where $\tau > 0$ is a time delay and $\mathbf{x}^*$ is a fixed point. For perturbations around $\mathbf{x}^*$, the eigenvalues Λ are solutions to

$$\mathrm{Det}[\mathbf{A} + e^{-\Lambda\tau}\mathbf{B} - \Lambda\mathbf{I}] = 0, \tag{25}$$

where $\mathbf{A} \equiv \partial\mathbf{F} \big/ \partial\mathbf{x}(t)|_{\mathbf{x}=\mathbf{x}^*}$, $\mathbf{B} \equiv \partial\mathbf{F} \big/ \partial\mathbf{x}(t-\tau)|_{\mathbf{x}=\mathbf{x}^*}$, and $\mathbf{I}$ is the identity matrix. Performing an analogous calculation for the system of equations (16) yields the following equation (where the asterisks have been suppressed for ease of notation):

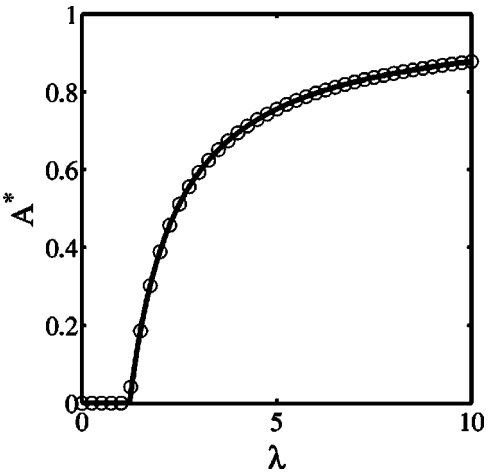

FIG. 1. Steady-state area as a function of λ when $\theta=5$. Analytic results of Eq. (17) (solid line) are compared to results from a time difference solver of Eq. (9) (open circles) using 10^2 grid points in radius space.

$$\mathrm{Det}\begin{bmatrix} -1-\Lambda & \lambda(1-A_j-2\pi p_a) & -\lambda p_a & 0 \\ 0 & -1-\Lambda+\lambda e^{-1/\theta}(1-A_j-2\pi p_a)e^{-\Lambda/\theta} & -\lambda e^{-1/\theta}p_a e^{-\Lambda/\theta} & 0 \\ 0 & -\pi\lambda e^{-1/\theta}(1-A_j-2\pi p_a)e^{-\Lambda/\theta} & -1-\Lambda+\pi\lambda e^{-1/\theta}p_a e^{-\Lambda/\theta} & \theta \\ 2\pi\theta & -2\pi\theta-2\pi\lambda e^{-1/\theta}(1-A_j-2\pi p_a)e^{-\Lambda/\theta} & 2\pi\lambda e^{-1/\theta}p_a e^{-\Lambda/\theta} & -1-\Lambda \end{bmatrix} = 0. \quad (26)$$

After some algebra, we find that two roots of this characteristic equation are $\Lambda=-1$, only one of which may be factored out. The simplified form of the characteristic equation is

$$0=(1+\Lambda)[(1+\Lambda)^3-\lambda e^{-1/\theta}(1-A_j)(1+\Lambda)^2 e^{-\Lambda/\theta} - \pi\lambda p_a e^{-1/\theta}(2\theta^2+2\theta(1+\Lambda)-(1+\Lambda)^2)]. \quad (27)$$

Consider the situation with fixed θ and increasing λ. If the nontrivial fixed point is to become unstable, it must do so via an oscillatory solution, as is usually the case for the instability of the persistence state of time-delay differential equations [23]. The transition from stability to instability takes place when $\Lambda=i\omega$. We solve for this crossing point by numerical evaluation of Eq. (27) for fixed θ and increasing λ. In this way, we are able to pick out the critical $\lambda_c(\theta)$. An alternative numerical criterion for finding the onset of a time-delay induced instability is developed in Ref. [23].

The phase diagram for the region $0.2\leqslant\theta\leqslant 100$ is shown in Fig. 2. There are a number of interesting aspects of this phase diagram. Notice that for every value of θ there is a critical λ_c where the system will exhibit oscillations. The physical reason behind these oscillations is simple. If the system produces too many young, it eventually reaches a point where the total density exceeds unity, and adults are unable to produce more seedlings. The density then drops to a level where young can be produced. However, this period of barrenness introduces a gap in the size structure which eventually leads to over-reproduction and recurring oscillations. Note also that when $\theta\gg 1$, the region over which the equilibrium fixed point is stable grows monotonically with θ. This implies that even in fast growing systems over-reproduction leads to instability of the steady state.

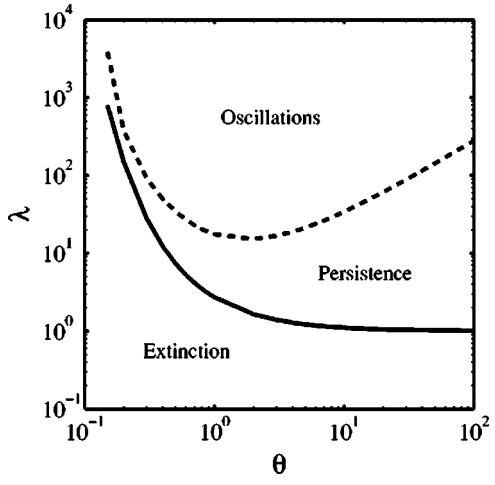

FIG. 2. Phase diagram of the mean field theory of the contact process with ontogeny defined in Eq. (9). The solid curve is the analytical line $\lambda=e^{1/\theta}$ separating extinction from persistence. The dashed curve separating persistence from oscillations derives from a numerical solution to the stability criteria in Eq. (27).

It is important to point out that, technically, the oscillating phase is a spurious consequence of ignoring collisions in the development of the mean field theory. However, it does point to the intriguing possibility that a competitively induced transition might exist in a spatial implementation of the contact process with ontogeny.

IV. SPATIALLY EXPLICIT SIMULATIONS: CONTACT PROCESS WITH ONTOGENY

In this section, we present results from Monte Carlo simulations of the contact process with ontogeny. We first present an overview of the types of steady-state behavior found in the model. We then present evidence that the phase transition of the contact process with ontogeny obeys the same critical dynamics as the simple contact process. We then show that the onset of a "ring-like" phase may be characterized by a growing peak in the radial distribution function. Throughout this section, we point out where and how the dynamics of a contact process with ontogeny differs from expectations of mean field theory.

Before we discuss the steady state, we mention briefly some of the details related to the numerical simulation. The region over which a growing organism extends may be approximated by a connected cluster of lattice sites or assigned explicitly in an off-lattice simulation. We are motivated by computational simplicity and physical transparency in choosing an off-lattice approach to incorporate ontogeny into the contact process. Monte Carlo simulations are conducted in a continuum of size $L\times L$ with periodic boundary conditions. The dynamics follow the model prescribed in Sec. II. All simulations are conducted with asynchronous event queues, where a particle may either die, disperse offspring, or collide with adjacent particles. Particles only grow when they have radius $r<1$ and when they are not in contact with any other particles. We validate the continuum approach by calculating the phase transition for an off-lattice contact process without ontogeny. We confirm that the phase transition in a continuum contact process is in the same universality class as directed percolation (DP) [4]. We also find that the critical reproductive value is $\lambda_c=2.015\pm0.005$. Note that λ_c for the continuum contact process is approximately 22% larger than that for the simple lattice contact process for which $\lambda_c\approx 1.645$ [3]. In fact, λ_c for the off-lattice contact process is equivalent to that of a lattice contact process model where

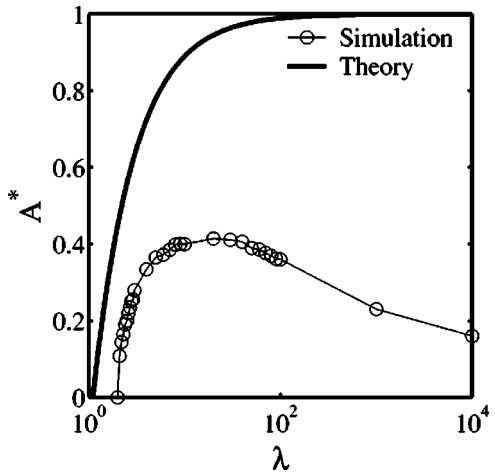

FIG. 3. Steady-state fractional area for $\theta=5$ with varying λ. Results from simulations of 32×32 systems (open circles with lines) are compared to mean field theory A^* (solid line). Mean field theory fails to capture the unimodal dependence of A^* on λ.

approximately 15% of lattice sites are unavailable for dispersal [24]. Having established the viability of the continuum approach, we now turn back to a discussion of the model.

A. Steady-state behavior

The conventional expectation in contact process-type models is that increasing reproduction leads to increasing steady-state density. In a contact process with ontogeny, reproduction introduces an ecological cost as a consequence of competition amongst offspring for limited space to mature. Such competition is in line with empirical findings on the growth of seeds in space-limited stands [9,25]. More generally, this model may be seen as typifying the competition for locally structured, limited resources, whether spatial or otherwise, which impacts all those who depend on them in a deleterious fashion. Below, we point out some of the features of the model, including a nonmonotonic relationship between the basal area and reproductive rate as well as the failure of mean field theory to reproduce the form of the size-structure distribution.

We calculate the steady, state basal area, $A^*(\lambda)$, of Monte Carlo simulations and find that $A^*(\lambda)$ is *unimodally* related to λ. Results from a suite of 32×32 simulations are compared to mean field theory (17) in Fig. 3. The mean field theory developed in Sec. III neglects interparticle competition and as such fails to capture the essential dynamics leading to the turnover of density with increasing reproduction. We have found evidence of this unimodal curve for varying θ and varying L. In fact, we believe that there is always a $\lambda_m(\theta)$, for which $A^*(\lambda)$ reaches a maximum, where $e^{1/\theta}<\lambda_m(\theta)<\infty$. We have insufficient numerical evidence to prove this claim, as yet. Of additional interest is the shape of the curve, $\lambda_m(\theta)$, particularly in the limits $\theta\to0$ and $\theta\to\infty$; does mean field theory predict this asymptotic shape?

The turnover of density with reproduction begs the question, how does such a unimodal curve come about? When reproduction is low ($\lambda\gtrsim e^{1/\theta}$), interparticle collisions are unlikely and the steady state is composed of a dilute collection of particles. As reproduction (λ) increases, so too does the likelihood that juvenile particles interfere with each other's growth. The continuous size distribution $\rho(r,t)$ shows a monotonic decline in density with r, with a discontinuity at $r=1$. Finally, as reproduction becomes very large ($\lambda\gg e^{1/\theta}$), most juvenile particles are unable to grow to maturity because of competition with other offspring. Adults generate a ring of seedlings which retards the spread of a population and limits its overall basal area. A depiction of the steady-state dynamics for $\theta=5$ and $\lambda=3$, 5, 20, and 500 is found in Fig. 4. Notice that the fraction of juveniles increases steadily with λ, whereas mean field theory predicts an asymptotic approach to a constant fraction when $\lambda\gg\lambda_c$. Also note the development of ring-like structures that are formed when $\lambda=500$ as a consequence of excessive reproduction. Even when the founding adult has died, the ring remains, with a hole at its center.

As is evident from this discussion of steady-state behavior, the contact process with ontogeny displays a rich variety of behavior. Much of this richness is due to the continuous size distribution, $\rho(r,t)$, which characterizes the model with an infinite number of order parameters. When competition is unimportant, $\rho(r,t)\approx\rho(0,t)e^{-r/\theta}$ for $r<1$, however, this stable size distribution is modified due to competition. We continue to seek out generalized forms to describe the nontrivial size distributions found in steady state.

B. Phase transition between life and death

The boundary between extinction and persistence is found by looking for power-law behavior in the survival distribution $P(t)$, number density $n(t)$, and spreading rate $R^2(t)$ as λ is varied [26]. We typically use 10^4 to 2×10^5 ensembles for each parameter value. All simulations begin with a single initial adult and are conducted with particle lists to rule out finite-size effects. The phase boundary derived from mean field theory is compared to that found in numerical simulations in Fig. 5.

What is the nature of this transition? The dynamics of a contact process with ontogeny may be likened to that of a non-Markovian contact process [4,27–31]. The introduction of a juvenile period implies that the dynamics at a time t depend on behavior at an earlier time $t-\tau$ where $\tau=1/\theta$. The critical behavior of different types of non-Markovian contact process have been shown to agree [29] and disagree [28] with the directed percolation universality class [4]. In the process of deriving the phase boundary, we also compare the dynamical critical exponents with those of directed percolation.

Via extensive numerical simulation, we find no evidence to suggest that the critical behavior of the contact process with ontogeny differs from that of directed percolation. We use the method of local slopes to estimate critical exponents as $t\to\infty$ [32]. For example, consider the survival probability, $P(t)\propto t^{-\delta}$. Because $P(t/b)\propto b^{\delta}t^{-\delta}$, we may write the local exponent as

$$\delta(t)=\frac{\log(P(t)/P(t/b))}{\log b}. \tag{28}$$

In Fig. 6, we estimate δ, η, and z, the critical exponents of $P(t)$, $n(t)$, and $R^2(t)$, respectively. Local slopes are measured

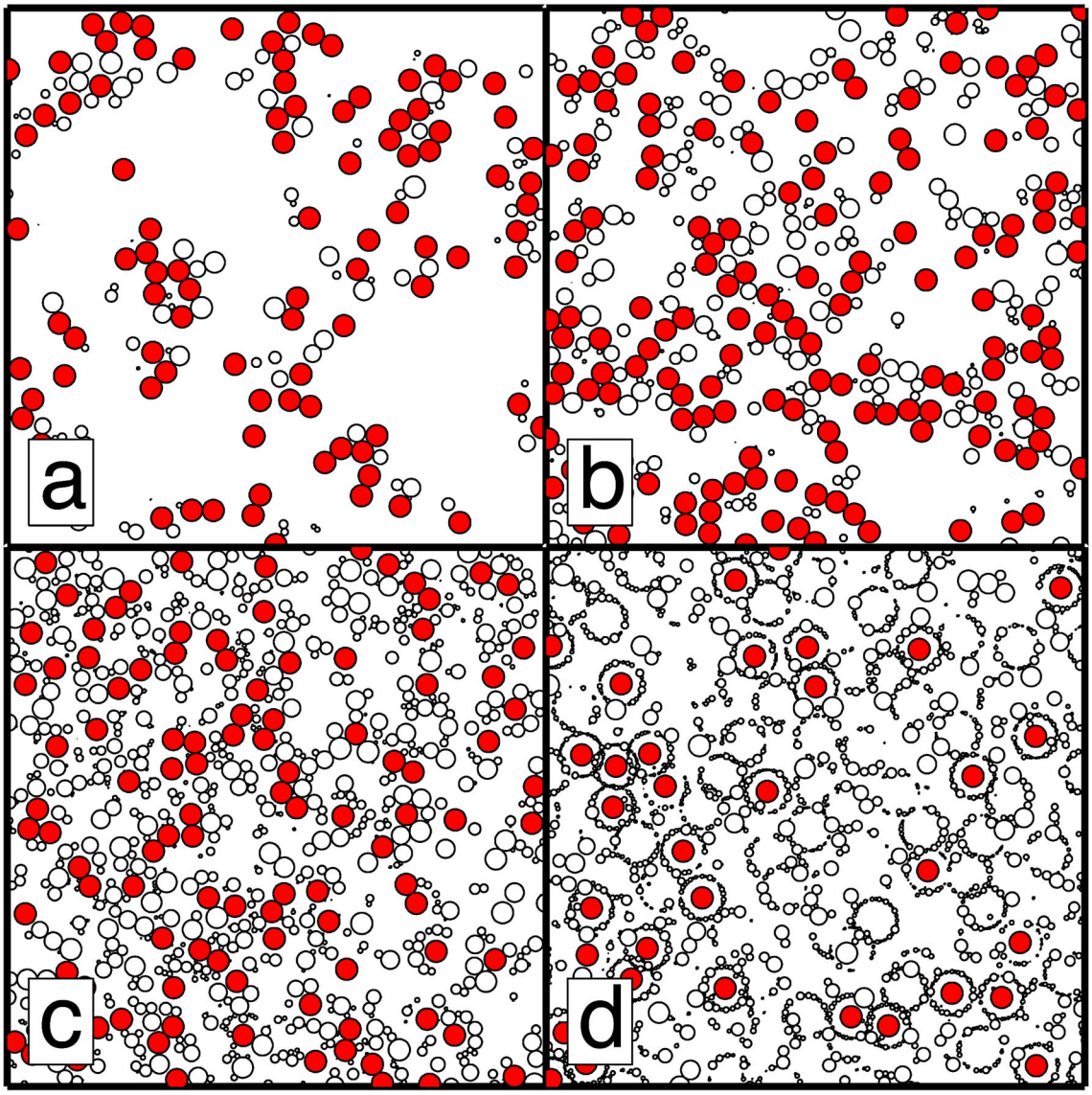

FIG. 4. Snapshot of steady-state behavior of a 50×50 system for $\theta=5$ and $\lambda=3$, 5, 20, and 500 for plots (a)–(d), respectively. Open circles represent juveniles for whom $r<1$ and shaded circles represent adults with $r=1$. Notice the presence of juvenile particle rings around adult particles at $\lambda=500$.

with $b=10$. Monte Carlo simulations with $\theta=10$ and $\lambda=1.978$, 1.980 and 1.982 lead to the prediction that $\lambda_c(\theta=10)=1.980\pm0.001$, as well as

$$\delta=0.44\pm0.01, \qquad \eta=0.235\pm0.01, \qquad z=1.125\pm0.01. \tag{29}$$

These values are in agreement with estimates of DP critical exponents [32] and bear out the scaling relation [26],

$$4\delta+2\eta=dz. \tag{30}$$

Similar values are obtained for the entire transition line shown in Fig. 5.

In the region $\theta<1$, we continue to seek out accurate determinations of the phase boundary line as well as its critical exponents. The rapid increase of the minimum bound on critical reproductive rate, $\lambda=e^{1/\theta}$ for $\theta<1$, hampers any attempt at extensive numerical simulation.

C. Onset of the ring-like phase

As pointed out in Sec. IV A, the competition between particles implies the steady state may either exist in a dilute or ring-like phase. Given a fixed dimensionless growth rate θ, we are interested in quantifying the onset of the ring-like phase as a function of λ. In the dilute phase, the system is characterized by chains of connected adults and isolated juveniles. Whereas in the ring-like phase, each adult particle produces a ring of juvenile particles which impede their and their progenitor's continued spread. We attempt to distinguish these situations by analyzing the spatial autocorrelation function of particle centers.

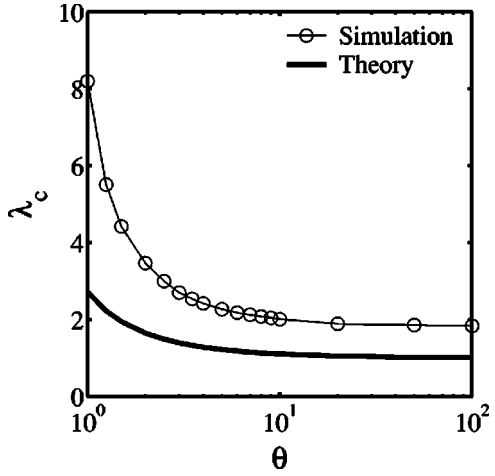

FIG. 5. Phase boundary between extinction and persistence. Results from simulations (open circles with line) are compared to mean field theory $\lambda_c = e^{1/\theta}$ (solid line).

We define the radial distribution function as [33]

$$g(r) = \frac{2V}{N^2}\left\langle \sum_{i<j} \delta(r - |\boldsymbol{x}_i - \boldsymbol{x}_j|) \right\rangle, \tag{31}$$

where V is the continuum volume, N is the number of particles, and $|\boldsymbol{x}|$ denotes the absolute magnitude of a vector. The definition of $g(r)$ implies that $2\pi\rho g(r) r dr$ is the mean number of particles in an annulus of radius r and width dr surrounding an arbitrary particle. We may estimate $g(r)$ from Monte Carlo simulations by taking a histogram of particle–pair separations. If we denote h_n as the number of particle pairs with separation between r_n and $r_n + \Delta r$, then for a simulation with unit area and particle density ρ,

$$g(r_n) = \frac{h_n}{\pi\rho^2 r_n \Delta r}. \tag{32}$$

If particles are distributed uniformly, then $g(r) \approx 1$. Deviations from unity indicate correlations in the spatial distribution of particles at different length scales. We calculate the radial distribution function, $g(r)$ for simulations with $\theta = 10$ and $\lambda = 5$ and $\lambda = 100$; the results are found in Fig. 7. Notice that both simulations have a peak in $g(r)$ at $r = 2$ which derives from particle chains. The peak at $r = 4$ and $r = 0$ is due to the ring of juvenile particles that surrounds adult particles or holes in the ring-like phase. The shape of the peak has a discontinuity of the form $(1 - r^2/16r_a^2)^{-1/2}$ at $r = 4r_a$. A uniform distribution of particles on a ring of radius $r = 2r_a$ has the same structure. The discontinuity reflects sweeping through larger and larger regions of angle with infinitesimal increases of distance close to the maximal separation $r = 4r_a$.

The use of the radial distribution function suggests the possibility of defining a structural order parameter that reflects correlations. In this way, a phase transition between dilute and ring-like states could be determined in a quantitative fashion.

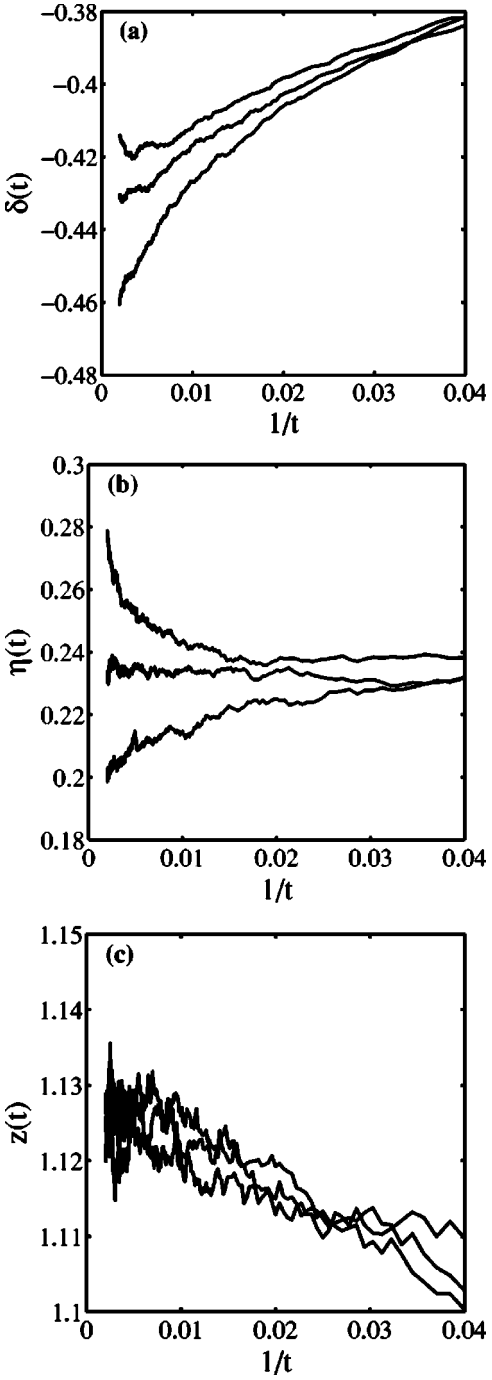

FIG. 6. Local slope measures of the critical exponents, δ, η, and z corresponding to the behavior of $P(t)$, $n(t)$, and $R^2(t)$ near the critical point. All simulations are at $\theta = 10$ with $\lambda = 1.978$, 1.980, and 1.982 corresponding to the curves from bottom to top. In (a) and (b), 2×10^5 ensembles were used while in (c) 10^5 ensembles were used. In all cases, the time is in dimensionless units.

V. GENERALIZATIONS OF THE MODEL

Our conception of the contact process with ontogeny as laid out in Sec. II leaves room for modifications with specific ecological applications in mind. For example, size-dependent fecundity, $c(r)$ or mortality $m(r)$ will alter the mean field condition separating life from death. In accord with other

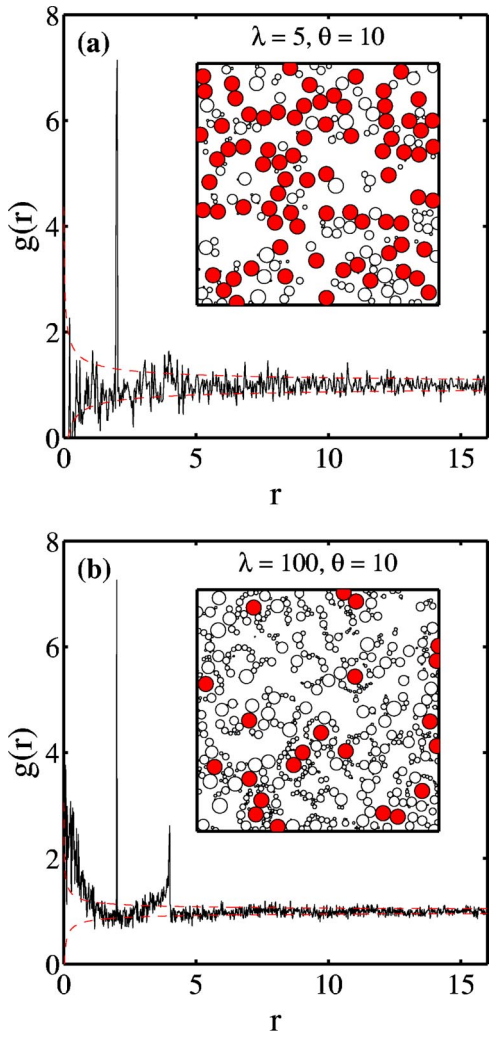

FIG. 7. Radial distribution function $g(r)$ measured for snapshots of Monte Carlo simulations in a 32×32 continuum, where r is in units of the adult radius. In (a), $\lambda=5$, $\theta=10$, and the single peak at $r=2$ corresponds to the contact between particles. In (b), $\lambda=100$, $\theta=10$, and there is an additional set of peaks at $r=0$ and $r=4$ corresponding to the correlation amongst juveniles (open circles) on the ring surrounding an adult particle (shaded circles) or hole. The dashed lines in the main figure represent the error bounds on $g(r)$ for uniformly distributed particles with density ρ. Deviations above or below this line indicate the presence of significant correlations or anti-correlations, respectively, in the actual distribution.

work on age-structured populations [19], the appropriate condition for instability of the absorbing state then becomes

$$\int_0^\infty dr c(r) e^{-\int_0^r dr' m(r')/\epsilon} > 1, \tag{33}$$

where ϵ is the growth rate. This condition reflects the presence of a stable size distribution

$$\frac{\rho^*(r)}{\rho^*(0)} = e^{-\int_0^r dr' m(r')/\epsilon}. \tag{34}$$

When $c(r)=\lambda\delta(r-1)$ and $m(r)=m$, the stability condition for general demographic schedules in Eq. (33) reduces to the condition derived in Sec. III, i.e., $\lambda > e^{1/\theta}$. Do all such demographic schedules leave unchanged the critical exponents of the phase transition?

To facilitate such an analysis, we construct a simple lattice analog of the contact process with ontogeny. The model, a time-delayed contact process (TDCP), is identical to that of the simple contact process [3,5], except that particles cannot reproduce until a time τ after being deposited on a lattice site. Near the critical point, collisions between offspring of the same adult are unlikely and the presence of ontogeny acts as a time delay between conception and maturation. We therefore consider the TDCP as representative of the dynamics of the contact process with ontogeny near the phase boundary. The model dynamics may be described in terms of the overall density, $p(t)$, and the density of adults, $p_a(t)$:

$$p'(t) = \lambda p_a(t)(1-p(t)) - p(t), \tag{35}$$

$$p_a'(t) = \lambda e^{-\tau} p_a(t-\tau)(1-p(t-\tau)) - p_a(t). \tag{36}$$

The phase boundary between life and death in the TDCP is $\lambda > e^{\tau}$, identical to the contact process with ontogeny. Preliminary analysis of the phase boundary of the TDCP indicates that it is in the same universality class as DP.

Finally, a spatial implementation of the contact process with ontogeny can accommodate problems with different dispersal kernels, growth rates, or competition structure. Here, we point out here one such modification. We modify the spatial model of Sec. IV so that particles are reproduced in the annulus $2r_a \leqslant r \leqslant 4r_a$. Simulations of this model at fixed θ and increasing λ show a transition from a dilute to a ring-like phase as well as a unimodal dependence of A^* on λ. This suggests that the ecological cost of increasing reproduction is a generic property of a contact process with ontogeny that has local dispersal and spatially exclusive interactions.

VI. CONCLUSIONS

Ontogeny in plants and trees is marked by the physical growth of sessile organisms over many orders of magnitude. During this period, seedlings develop into adults capable of reproduction. This maturation is not inevitable. In fact, the norm for many plants is the failure of seedlings to become viable adults. Density-dependent competition inhibits the maturation of seedlings and can even lead to adverse effects on plants/trees which produce too many offspring.

In this paper, we extended the simple contact process to model the transition between juvenile and adult states. We presented a general scheme for studying contact processes with ontogeny in Sec. II. We then derived a size-structured mean field theory which predicts the presence of an oscillatory phase given increasing reproduction. The presence of oscillatory steady states is common in models of systems with time delays [19,22,34]. However, the oscillatory steady-state depends on a coherent global response to changes in density, a condition unlikely to be satisfied by a spatial model.

Indeed, we find that steady-state dynamics from Monte Carlo simulations differ greatly from the predictions of mean field theory. For example, the total area taken up by particles

is unimodally related to reproduction λ, given a fixed growth rate θ. The ecological cost of reproduction is not prescribed by the model, rather it emerges naturally from the competition for limited space.

We also find that increasing reproduction moves the system from a dilute phase to a ring-like phase. Examples of ring-like formations in ecology can be found in the clustering of redwoods. The formations called "fairy rings" or "family circles" are a consequence of clonal sprouting, i.e., reproductive events that are in contact with the mother tree [35–37].

Other models of size-structured competition have been studied and solved [20–22,38,39], but none have been developed with the contact process in mind. The contact process and its variants [2–5,8,40] are the standard phenomenological tools for modeling stochastic spatial ecologies. This work makes it possible to use the contact process to study how organisms which take up space, in addition to living in space, affect ecosystem structure and dynamics.

ACKNOWLEDGMENTS

The authors thank Mika Latva-Kokko and Alex Lobkovsky for helpful discussions. They also thank Jack Wisdom for the use of a Beowulf cluster in which much of the numerical work was completed. This work was supported in part by the National Science Foundation Grant No. DEB-0083983.

[1] T. M. Liggett, *Interacting Particle Systems* (Springer, New York, 1985).
[2] R. Durrett, SIAM Rev. **41**, 677 (1994).
[3] J. Marro and R. Dickman, *Nonequilibrium Phase Transitions in Lattice Models* (Cambridge University Press, Cambridge, UK, 1999).
[4] H. Hinrichsen, Adv. Phys. **49**, 815 (2000).
[5] T. Harris, Ann. Prob. **2**, 969 (1974).
[6] D. Tilman, Ecology **75**, 2 (1994).
[7] C. Neuhauser, J. Theor. Biol. **193**, 445 (1998).
[8] S. P. Hubbell, *The Unified Neutral Theory of Biodiversity and Biogeography*, No. 32 in Monographs in Population Biology (Princeton University Press, Princeton, NJ, 2001).
[9] J. White and J. L. Harper, J. Ecol. **58**, 467 (1970).
[10] M. G. Neubert and H. Caswell, Ecology **81**, 1613 (2000).
[11] T. Caraco *et al.*, Am. Nat. **160**, 348 (2002).
[12] W. S. C. Gurney, D. C. Speirs, S. N. Wood, E. D. Clarke, and M. R. Heath, J. Anim. Ecol. **70**, 881 (2001).
[13] T. Hara, J. Theor. Biol. **109**, 173 (1984).
[14] T. Hara, J. Theor. Biol. **110**, 223 (1984).
[15] T. Kohyama, Ann. Bot. (London) **68**, 173 (1991).
[16] P. R. Moorcroft, G. C. Hurtt, and S. W. Pacala, Ecol. Monogr. **71**, 557 (2001).
[17] A. G. McKendrick, Proc. Edinburgh Math. Soc. **44**, 98 (1926).
[18] H. von Foerster, in *The Kinetics of Cellular Proliferation*, edited by F. Stohlman (Grune and Stratton, New York, 1959).
[19] J. D. Murray, *Mathematical Biology*, 2nd ed. (Springer, Berlin, 1993).
[20] J. A. J. Metz and O. Diekmann, *The Dynamics of Physiologically Structured Populations*, Lecture Notes in Biomathematics (Springer, Berlin, 1986).
[21] J. M. Cushing, *An Introduction to Structured Population Dynamics* (SIAM, Philadelphia, 1998).
[22] W. S. C. Gurney and R. M. Nisbet, *Ecological Dynamics* (Oxford University Press, New York, Oxford, 1998).
[23] E. Beretta and Y. Kuang, SIAM J. Math. Anal. **33**, 1144 (2002).
[24] A. G. Moreira and R. Dickman, Phys. Rev. E **54**, R3090 (1996).
[25] K. Yoda, T. Kira, H. Ogawa, and K. Hozumi, J. Biol. Osaka City Univ. **14**, 107 (1963).
[26] P. Grassberger and A. de la Torre, Ann. Phys. (N.Y.) **122**, 373 (1979).
[27] P. Grassberger, H. Chate, and G. Rousseau, Phys. Rev. E **55**, 2488 (1997).
[28] R. Cafiero, A. Gabrielli, and M. A. Munoz, Phys. Rev. E **57**, 5060 (1998).
[29] R. Gerami, Phys. Rev. E **65**, 036102 (2002).
[30] S. Dorogovtsev and J. Mendes, Phys. Rev. E **63**, 046107 (2001).
[31] S. Trimper and K. Zabrocki, Phys. Lett. A **321**, 205 (2004).
[32] C. A. Voigt and R. M. Ziff, Phys. Rev. E **56**, R6241 (1997).
[33] D. C. Rapaport, *The Art of Molecular Dynamics Simulation* (Cambridge University Press, Cambridge, U.K., 1997).
[34] R. M. May, *Stability and Complexity in Model Ecosystems* (Princeton University Press, Princeton, NJ, 1974).
[35] J. Rydelius and W. Libby, in *Clonal Forestry II*, edited by M. Ahuja and W. Libby (Springer, Berlin, 1993), pp 158–168.
[36] R. Noss, ed., *The Redwood Forest: History, Ecology, and Conservation of the Coast Redwoods* (Island Press, Washington, D.C., 2000).
[37] D. Rogers, Can. J. Bot. **78**, 1408 (2000).
[38] J. M. Cushing, SIAM (Soc. Ind. Appl. Math.) J. Appl. Math. **49**, 838 (1989).
[39] S. A. L. Kooijman, *Dynamic Energy and Mass Budgets in Biological Systems* (Cambridge University Press, Cambridge, UK, 2000).
[40] J. Chave, H. C. Muller-Landau, and S. A. Levin, Am. Nat. **159**, 1 (2002).
[41] Note that there is no factor of r^2 for $r>1$ because all particles with radius "r" actucally have unit radius.